

Field Emission From Carbon Nanotubes Grown On Line-patterned Cathode Electrodes

B.K. Kim, B.Y. Kong, J.Y. Seon, N.S. Lee

Dept. of Nano Science and Technology, Sejong University, Gwangjin-Gu, Seoul, Korea

H.J. Kim, I.T. Han, and J.M. Kim

Samsung Advanced Institute of Technology, P.O. Box 111, Suwon, Korea

Phone: 82-2-3408-3786, E-mail: nslee@sejong.ac.kr

Abstract

We investigated field emission (FE) characteristics of multi-walled carbon nanotubes (CNTs) grown on all over patterned cathode electrode lines (CL pattern) and grown on along the central areas of the cathode lines (SL pattern). The CNTs grown on the SL pattern showed a lower threshold voltage and higher emission current than those on the CL pattern, due to the concentration of electric fields at the edges of the cathode lines. For the SL-patterned CNTs, however, the FE gradually spread out to the neighbors with time, and was instantly extinguished in some area and then slowly resumed again. Such areal-spread FE did not occur for the CL-patterned sample, leading to the stable FE together with the instant turn-on capability. It is suggested that the spread FE and instability for the SL-patterned CNTs may be related to the electrical charging on the insulator surface around the cathode line edges.

1. Introduction

Carbon nanotubes (CNTs) have attracted considerable attention as an electron emitter material especially for field emission displays (FEDs),^[1-3] due to their excellent properties such as high aspect ratios, high mechanical strength, and chemical stability. Field emitters using CNTs have been fabricated by various methods including screen printing,^[4] micro-contact printing,^[5] Doctor blading,^[6] and electrophoresis^[7] of particulate CNTs, and direct growth of CNTs by chemical vapor deposition (CVD).^[8] The CNT FEDs have also been fabricated in a diode^[6,9] or triode structure^[10]. For the diode-structured emitter arrays, a simple matrix type^[9] and an active matrix type controlled by thin film transistors,^[6] have been attempted. The CNT emitter arrays with the triode structure have been devised to have an upper-gate^[11] or under-gate type.^[12] In the diode structure^[6,9] and the under-gate type triode structure^[13], electrons are strongly emitted from the CNTs located at the edges of cathode electrode lines (CELs), due to the concentration of electric fields. Although real-working

FEDs have been demonstrated both in the diode and triode structures using this edge emission, its emission mechanism has not yet been fully understood. This study investigated field emission (FE) characteristics of diode type CNT emitters grown on an entire area and a central area of every CEL. Whether the CNTs are placed at the CEL edges or not had a great effect upon their field emission properties.

2. Experimental

CNTs were synthesized on glass substrates by thermal CVD. The 100 nm-thick Cr layer served as a cathode electrode and the 10nm-thick layer of 52%Fe-42%Ni-6%Co (Invar alloy) as a catalyst for CNT synthesis. After heating up to 580°C, the growth was performed for 30 min at 1 atm. using a mixture of CO (80 sccm) and H₂ (1270 sccm). To prepare substrates for the CNT growth, the cathode electrode and catalyst layers were line-patterned by photolithography. Fig. 1 shows two different types of line patterns: (1) the catalyst lines simply patterned to have the same width as the CELs (so-called, simple line (SL) pattern); (2) the catalyst lines patterned to be located along the central area of the cathode lines (so-called central line (CL) pattern). As-grown CNTs were characterized by SEM and TEM. FE characteristics of CNT emitters were measured in a diode configuration in a vacuum of $\sim 3 \times 10^{-6}$ torr. The indium tin oxide glass coated with ZnS:Cu,Al phosphor was used for the anode. The cathode-to-anode gap of 400 μm was kept by glass spacers. FE measurements were carried out using a high voltage power supply (Keithley 248) and a source-measure unit (Keithley 236). For the SL- and CL-patterned emitters with the diode structure, we simulated the electric potential distributions and electron trajectories using the commercial program SIMON.

3. Results and discussion

The CNTs grown only on the Invar catalyst in both SL and CL patterns exhibit almost identical

morphologies. As given in Fig. 1(c) and (d), the CNTs were $\sim 14 \mu\text{m}$ tall, and vertically aligned but microscopically crooked. The CNTs show a bamboo-like structure with relatively well-ordered graphitic walls parallel to the tube axis. Their inner and outer diameters are of 5~10 nm and 10~50 nm, respectively.

Although as-grown CNTs on both the SL and CL patterns exhibit almost the same morphologies, their FE characteristics are considerably different. In Fig. 2, the threshold electric fields (required for the emission of $1 \times 10^{-6} \mu\text{A}/\text{cm}^2$) are approximately 2.6 and 3.1 $\text{V}/\mu\text{m}$ for the SL and CL patterns, respectively. The emission of $1 \times 10^{-5} \mu\text{A}/\text{cm}^2$ are marked at 2.8 and 4.0 $\text{V}/\mu\text{m}$, respectively. The SL-patterned sample shows much higher FE current density all over the fields than the CL-patterned one. Using the Fowler-Nordheim relationship,^[13] we estimated the field enhancement factors β from the I-V curves. The β value in principle depends only on the geometrical shape of the emitters for a given work function. The β is defined as $E = \beta V/d$, where E is the effective local electric field just at the emitter tips, V the applied voltage, and d the cathode-to-anode gap. Assuming the work function of the CNTs to be the same as that of graphite, 5.0 eV, the β values are calculated to show similar values, 1380 and 1451, in the low electric field regions for the SL and CL patterns, respectively.

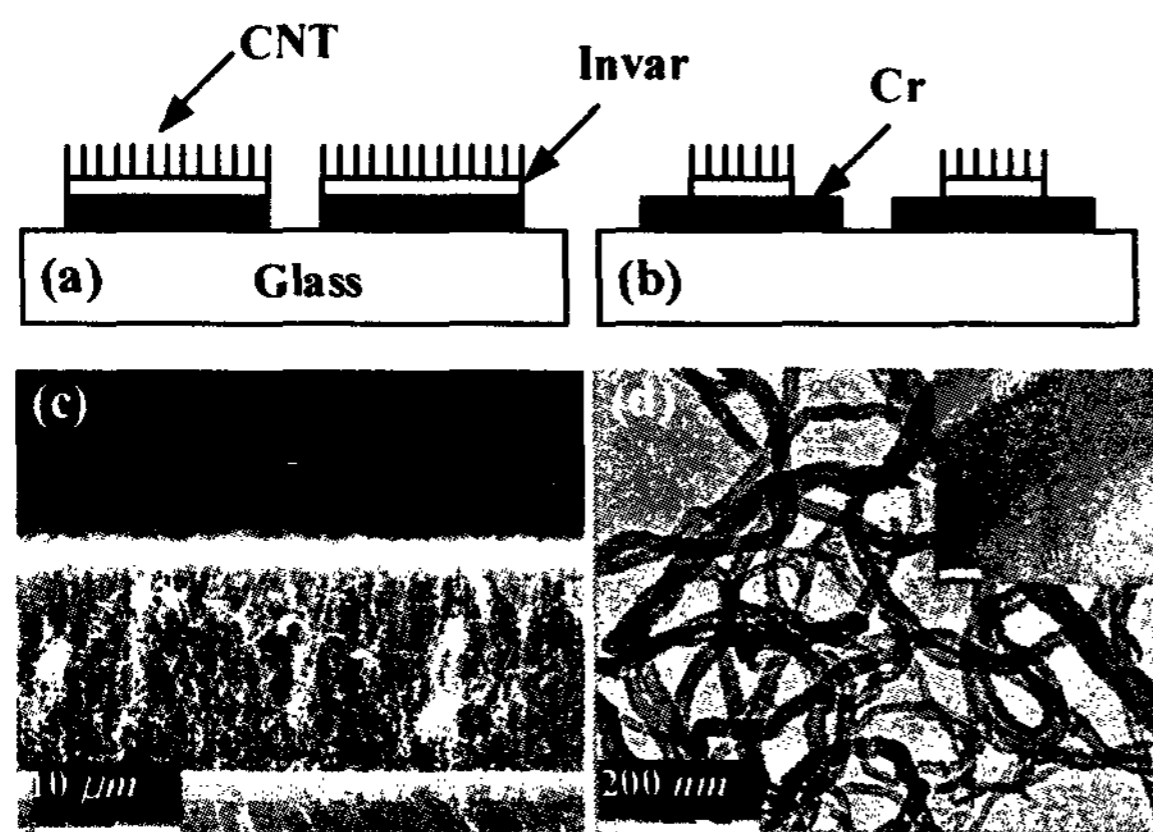


Fig. 1 Schematics of (a) SL- and (b) CL-patterned samples. The Cr CELs were 600 μm wide and the gap between adjacent CELs was 142 μm . For the CL pattern, the catalyst lines were centrally positioned 150 μm apart from both edges of each CEL. (c) SEM and (d) TEM images of CNTs both for the SL and CL patterns. An inset in (b) shows an HRTEM image with the scale bar of 5 nm.

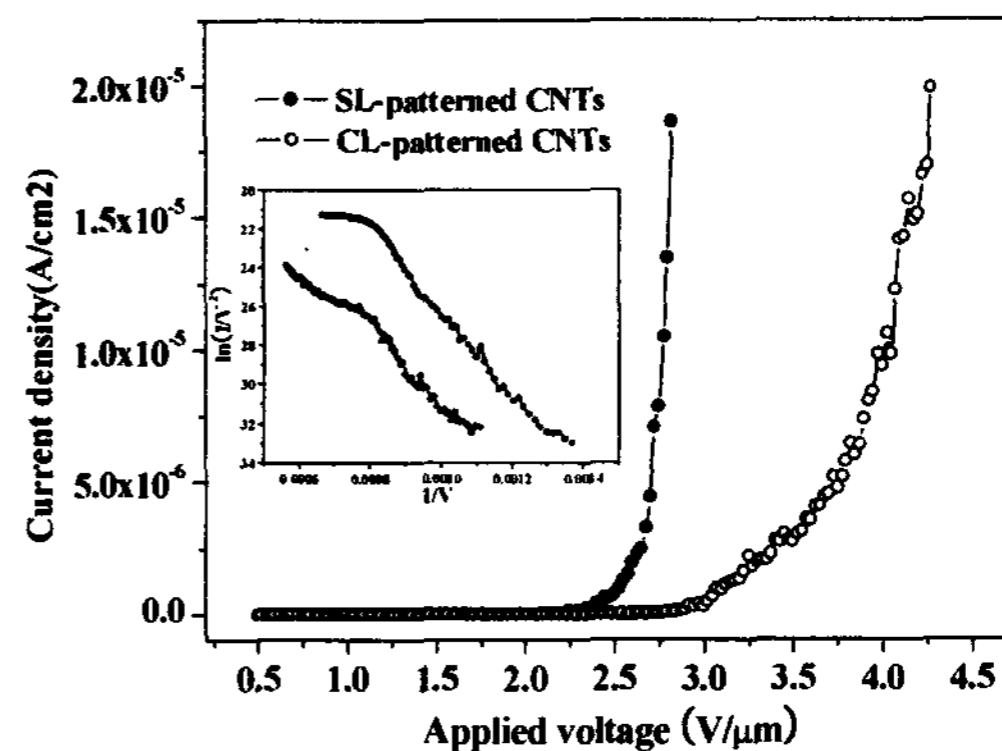


Fig. 2 FE I-V curves of CNTs with the SL and CL patterns, where the inset shows their corresponding Fowler-Nordheim plots.

To investigate the effect of the patterns on the FE characteristics, we calculated electric potential distributions and trajectories of emitted electrons around the CNT emitters for the SL and CL patterns, as presented in Fig. 3 (a) and (b). It is shown for both cases that equipotential lines are densely distributed at the CEL edges in lateral contact with the insulator region. For the SL pattern, the CNT emitters exist all over the CEL area including the edges, but along the central region 150 μm apart from both edges of each CEL for the CL pattern. For the SL pattern, such a concentration of electric fields at the edges would give rise to FE along them rather than in other area, likely leading to the FE at low threshold field. When only one CEL is turned on, therefore in the SL pattern, two lines are actually lit up on the phosphor, as shown in Fig. 3(c), due to the electron emission only from the CNTs on the both edges of the CEL. This can be understood by the electron trajectories given in Fig. 3(a). For the CL pattern, however, turning-on one CEL results in light emission as a line on the phosphor, implying the uniform electron emission all over the regions of CNT emitters, as demonstrated in Fig. 3(b) and (d).

With all CELs turned on for the SL pattern, the electron trajectories given in Fig. 3(a) indicates that electrons emitted from the two face-to-face edges of adjacent CELs hit the phosphor which is located just above the insulator area between the CELs. Thus the phosphor is luminescent as stripes whose locations laterally move half the CEL pitch from each CEL. This is presented in Fig. 4(a). Here the long arrows indicate the locations of the centers of the CELs, along which no luminescence is observed. In Fig. 3(a), the electrons emitted from the face-to-face edges of two

adjacent CELs are overlapped in the central part of the phosphor region where the electrons arrive. This would give rise to a brighter core line along each luminous stripe, as shown in Fig. 4(a).

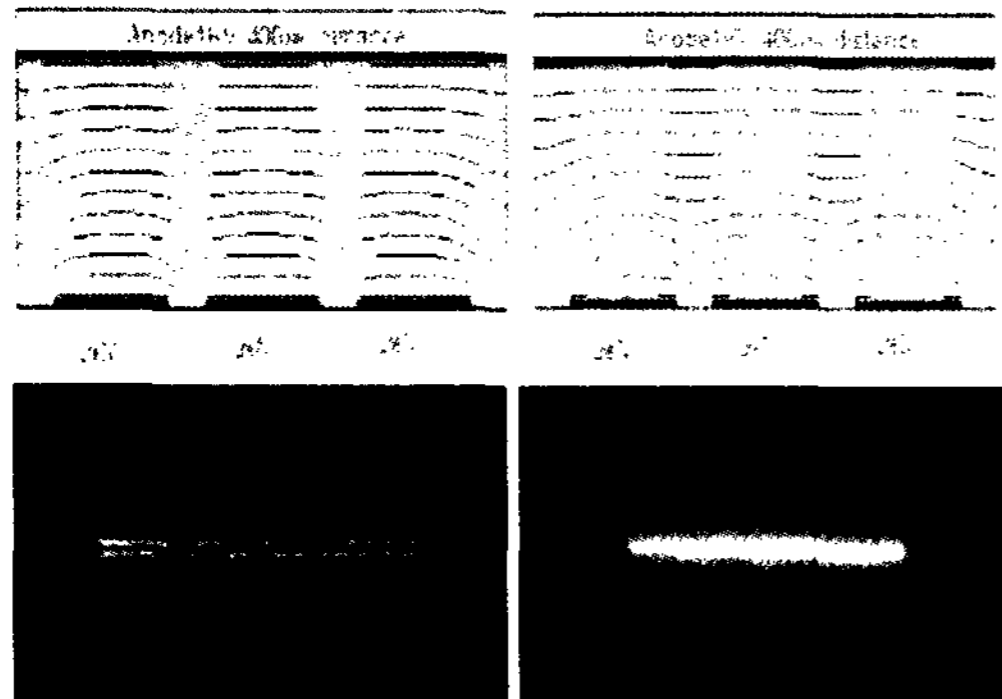


Fig. 3 Distribution of equipotential lines and trajectories of emitted electrons in (a) SL-patterned and (b) CL-patterned samples. (c) A phosphor emission image of two lines lit-up upon turning-on one CEL for the SL pattern and (d) one-line emission image for the CL pattern.

Simply from the I-V curves, the SL pattern seems to be better than the CL pattern in terms of the threshold field as well as the emission current. Observing emission images of the SL-patterned sample, however, the emission area gradually spread out to the neighbors with time upon applying a constant voltage to the anode. The anode was biased to the square-shaped pulse of 850V with the duty ratio of 1% at 60Hz. On applying the voltage, a partial area emitted light with the current of 20.5 μA over the 2" diagonal sample ((Fig. 4(b)). Thereafter, the emission area slowly spread out, reaching the current of 68.7 μA after 5 min ((Fig. 4(c)). This phenomenon was also observed with the application of dc voltages. At higher voltages, the emission area expanded faster with high currents. As soon as the same voltage was applied to the anode immediately just after turning off, the preceding emission image was restored. If the emission was turned off longer than several tens of seconds, however, the areal-spread emission occurred again as the anode was biased. From time to time, the emission was extinguished in some area at an instant and then resumed slowly again. The SL-patterned sample showed somewhat capacitive characteristics with a lack of the instant turn-on capability. For the CL-patterned sample, however, the spread emission was not observed, leading to the stable FE together with the instant turn-on performance.

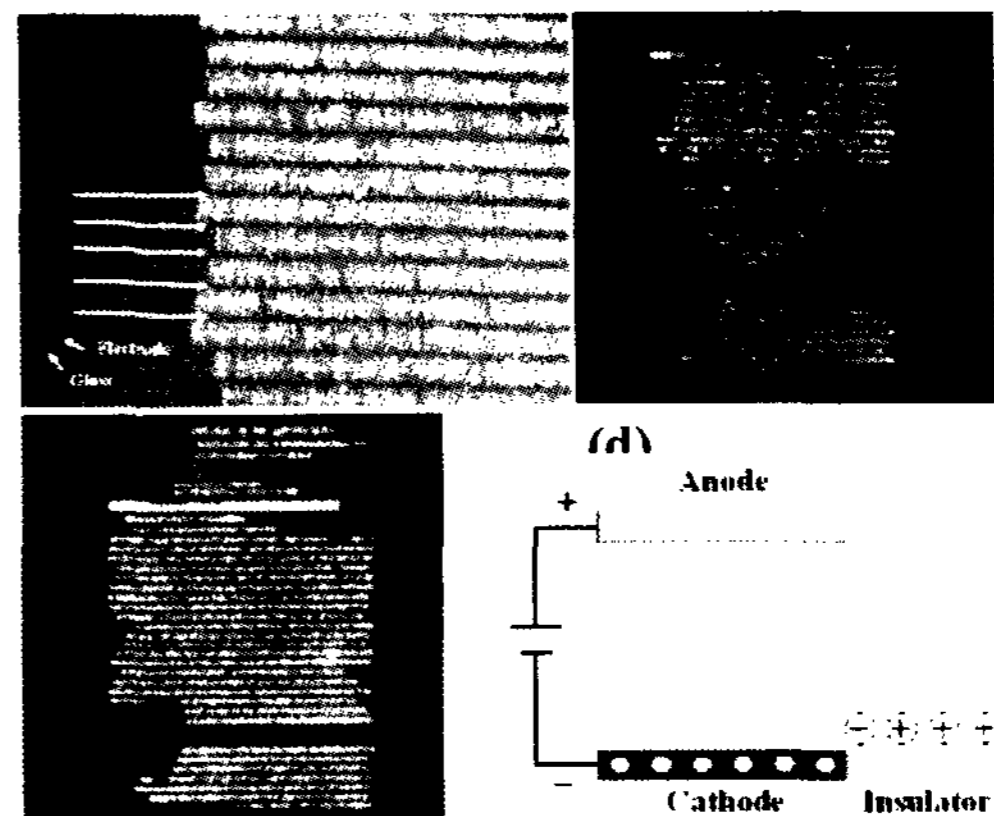


Fig. 4 (a) Phosphor emission image with all CELs turned on in the SL-patterned sample. Emission lines occur on the phosphor along the inter-CEL area (denoted as glass by an arrow) between adjacent CELs due to the edge emission. (b) Initial emission image with 20.54 μA and (c) spread emission image with 68.64 μA taken 5 min after (b). (d) Electrical charging mechanism of an insulator surface adjacent to the CEL.

A possible explanation of such phenomena is that the insulator region near to the CNT emitters is electrically charged up to affect their FE properties. Consider the insulator covering the cathode electrode in the dc glow discharge.^[14] Upon supplying a negative voltage to the electrode, the glow discharge will be initiated since the insulating surface is also negatively biased simultaneously. As the insulating surface begins to be bombarded by positive ions, the surface potential will rise towards zero, finally extinguishing the glow discharge. Since the insulator can be here regarded as a capacitor, it will take some time to charge up the insulator surface, $\sim 1 \mu\text{sec}$ in the typical dc sputtering condition. Coming back to our case, the cathode electrodes are laterally in contact with the insulator, as shown in Fig. 4(d). Upon applying a constant voltage above the threshold to the SL-patterned sample, electrons start to be emitted from some preferential positions on the edges due to the non-uniformity of the sample. The emitted electrons travel to the anode along the trajectories given in Fig. 3(a). During their journey, the electrons collide with residual gases existing on their paths, producing positive ions. The ions head downward likely along the paths opposite to the electron trajectories. Most of the ions bombard the edge areas of the CELs, but some electrons hit the insulator surface adjacent to the CEL edges. On the CELs, the

ions are neutralized, coming back to the molecular states, but the adjacent insulator surface starts to be charged up by the ions. Such a buildup of positive charges enhances the electric fields around the CEL edges, coupled together with the anode voltage. As the charge-up of the insulator surface near the emission edge advances, therefore, the emission area spread out along the edge. When the accumulated positive charges are discharged in an area, the emission would be extinguished there due to the instant decrease of the electric fields around the edge. Recharging the insulating surface makes the spread emission resume again. We suggest that the spread emission and instability for the SL-patterned case may be related to the electric charging on the insulating surface around the electrode edges.

4. Conclusion

The CNT emitters showed considerably different FE characteristics with the SL and CL patterns, in spite of their identical morphologies and structures. The SL-patterned CNTs possessed a low threshold field due to the edge emission, but revealed the unstable spread FE. It is suggested that the spread FE and instability of the SL-patterned CNTs may be attributed to an electrical charging on the insulator surface. However, the CL-patterned sample resulted in the stable FE with the instant turn-on performance.

5. References

1. W. A. de Heer, A. Chatelain, and D. Uzgate, *Science* 270, 1179 (1995).
2. W. Zhu, C. Bower, O. Zhou, G. Kochanski, and S. Jin, *Appl. Phys. Lett.* 75, 873 (1999).
3. L. Nilsson, O. Groening, C. Emmenegger, O. Kuettel, E. Schaller, L. Schlapbach, H. Kind, J-M. Bornard, and K. Kern, *Appl. Phys. Lett.* 76, 2071 (2000).
4. T. J. Vink, M. Gillies, J. C. Kriege, and H. W. J. J. van Laar, *Appl. Phys. Lett.* 83, 3552 (2003).
5. J-M. Bonard, M. Croci, C. Klinke, R. Kurt, O. Noury, and N. Weiss, *Carbon* 40, 1715 (2002).
6. J. H. Lee, Y. H. Lee, Y. R. Cho, S. Y. Kang, M. Y. Jung, C. S. Hwang, S. K. Lee, D. H. Kim, H. S. Um, K. I. Cho, and D. S. Ma, *Proceedings of the 7th International Display Workshops*, Kobe, Japan, 2000, p. 935.
7. W. B. Choi, Y. W. Jin, S. J. Lee, M. J. Yun, J. H. Kang, Y. S. Choi, N. S. Park, N. S. Lee, and J. M. Kim, *Appl. Phys. Lett.* 78, 1547-1549 (2001).
8. Z. F. Ren, Z. P. Huang, D. Z. Wang, J. G. Wen, J. W. Xu, J. H. Wang, L.E. Calvet, J. Chen, J. F. Klemic, and M. A. Reed, *Appl. Phys. Lett.* 75, 1086(1999).
9. N. S. Lee, D. S. Chung, J. H. Kang, H. Y. Kim, S. H. Park, Y. W. Jin, Y. S. Choi, I. T. Han, N. S. Park, M. J. Yun, J. E. Jung, C. J. Lee, J. H. You, S. H. Jo, C. G. Lee and J. M. Kim, *Jap. J. Appl. Phys.* 39, 7154 (2000).
10. M. A. Guillorn, A. V. Melechko, V. I. Merkulov, E. D. Ellis, C. L. Britton, M. L. Simpson, D. H. Lowndes, and L. R. Bayor, *Appl. Phys. Lett.* 79, 3506 (2001).
11. I.T. Han, H.J. Kim, Y.J. Park, N.S. Lee, J.E. Jang, J.W. Kim, J.E. Jung, J.M. Kim, *Appl. Phys. Lett.* 81, 2070 (2002).
12. Y. S. Choi, J. H. Kang, H. Y. Kim, B. G. Lee, C. G. Lee, S. K. Kang, Y. W. Jin, J. W. Kim, J. E. Jung, and J. M. Kim, *Appl. Surf. Sci.* 221, 370 (2004).
13. R. H. Fowler, L. W. Nordheim, *Proc. R. Soc. London Ser. A.* 119, 173(1928).
14. B. Champman, *Glow Discharge Processes* (Wiley, New York, 1980), p. 139.